

Abstract. We have obtained échelle spectroscopy of 14 Population II objects selected from those previously observed by Bonifacio & Molaro (1997). For one object, HD 140283, we obtained exquisite data with the High Dispersion Spectrograph on the Subaru Telescope, with S/N exceeding 1000 per 0.018 Å pixel. Li abundances have been determined by spectral synthesis from both the 6708Å resonance line and also from 6104Å subordinate feature. Firm detections of the weak line have been made in seven objects, and upper limits are reported for the remainder. Our 6708Å abundances agree with those reported by Bonifacio & Molaro at the 99%-confidence level. Abundances from the 6104Å line hint at a higher Li abundance than that determined from the resonance feature, but this evidence is mixed; the weakness of the 6104Å line and the large number of upper limits make it difficult to draw firm conclusions. NLTE-corrections increase (rather than eliminate) the size of the (potential) discrepancy, and binarity appears unlikely to affect any abundance difference. The effect of multi-dimensional atmospheres on the line abundances was also considered, although it appears that use of 3-D (LTE) models could again act to *increase* the discrepancy, if one is indeed present.

Key words: stars: abundances - stars: Population II - stars: interiors

Lithium 6104Å in Population II stars

A. Ford^{1,2}, R.D. Jeffries¹, B. Smalley¹, S.G. Ryan², W. Aoki³, S. Kawanomoto³, D.J. James^{4,5,6}, and J.R. Barnes⁴

¹ Department of Physics, Keele University, Keele, Staffordshire, ST5 5BG, UK

² Department of Physics and Astronomy, The Open University, Walton Hall, Milton Keynes, MK7 6AA, UK

³ National Astronomical Observatory of Japan, Mitaka, Tokyo, 181-8588 Japan

⁴ School of Physics and Astronomy, University of St Andrews, North Haugh, St Andrews, Fife, KY16 9SS, UK

⁵ Laboratoire d'Astrophysique, Observatoire de Grenoble, BP-53, F-38041 Grenoble, Cedex 9, France

⁶ Observatoire de Genève, Chemin des Maillettes, #51, Sauverny, CH-1290, Switzerland

email: alison.ford@open.ac.uk; rdj@astro.keeple.ac.uk; bs@astro.keeple.ac.uk; s.g.ryan@open.ac.uk; aoki.wako@noa.ac.jp; kawanomo@optik.mtk.nao.ac.jp; djames@obs.ujf-grenoble.fr

Received; accepted

1. Introduction

Population II stars are older and more metal-poor than the Pop. I stars which make up most of the Galactic disk. They are predominantly found in the Galactic bulge, in the spherical halo around the Galaxy, and in globular clusters, although they also make up $\sim 0.1\%$ of the population of nearby stars. They formed early in the life of the Galaxy, and therefore are better indicators of early Li abundances than their younger Pop. I counterparts. This seemed to be supported by the discovery of a Li abundance plateau in these objects by Spite & Spite (1982). The Spite plateau (Li abundance = $2.09^{+0.19}_{-0.13}$ dex, Ryan et al. 2000 – where $A(\text{Li}) = \log_{10} \frac{N(\text{Li})}{N(\text{H})} + 12$) includes objects in the temperature range $5600 \text{ K} \leq T_{\text{eff}} \leq 6400 \text{ K}$, and metallicity range $[\text{Fe}/\text{H}] < -1.3$. Since the plateau Pop. II stars are predicted to have undergone little Li depletion over the course of their lives (< 0.1 dex according to Ryan et al. 1999 – hereafter RNB99, ≤ 0.2 dex according to Pinsonneault et al. 1999, but possibly as high as 0.3 dex according to Salaris & Weiss 2001) the plateau Li abundance has been suggested to be close to the primordial Li abundance, Li_p . Recent work by RNB99 found that the plateau is ultra-thin, but slopes with metallicity ($\frac{d(A(\text{Li}))}{d[\text{Fe}/\text{H}]} = +0.118 \pm 0.023$), suggesting that the Galactic Li abundance increased slowly with metallicity during the time when Pop. II stars were forming. Li abundances in Pop. II stars cooler than the plateau are depleted. It is also possible that the plateau abundance is the result of stellar Li depletion from a higher value (see e.g. Pinsonneault 1997, 1999), though why the resulting Li abundance should then be so uniform in these objects is unclear (Théado & Vauclair 2001). Salaris & Weiss (2001) have developed models which include atomic diffusion (untem-

pered by mass loss) which they compare with the plateau $\text{Li}-T_{\text{eff}}$ trend. They conclude that this mechanism leaves the stars' Li abundances depleted by ~ 0.3 dex relative to their initial abundances. They comment that the neglect of both mass-loss and radiative-levitation processes in their models probably leads to this being an overestimation, but more work is required to quantify this. However, the Spite plateau is probably still the best indicator available (after consideration of, and correction for, effects such as diffusion) for the primordial Li abundance, and can still be used to set limits on cosmological parameters such as η (the baryon-to-photon ratio) and Ω_B (the universal baryon density).

There is yet another problem with assuming that the plateau abundance is the same as Li_p : the plateau abundance is derived from only one spectral line, the 6708Å resonance feature. Recent work by Kurucz (1995), Carlsson et al. (1994), Stuik et al. (1997), Uitenbroek (1998) and Asplund et al. (1999) has suggested that this line might be unrepresentative of the actual Li abundance within the stars, due to omissions in our understanding and modelling of stellar atmospheres. Recent works on halo stars (Bonifacio & Molero 1998, hereafter BM98 – and next subsection) and young cluster stars (Soderblom et al. 1993a; Russell, 1996; Ford et al. 2002) have used the weak (excitation potential = 1.8 eV) Li I subordinate line at 6104Å in addition to the 6708Å line (hereafter 6708 and 6104 are taken to mean 'the Li I line at 6708Å' and 'the Li I line at 6104Å' respectively), to attempt to determine Li abundances. This paper builds on those previous studies.

1.1. Multi-dimensional atmospheres: the story so far...

– Kurucz (1995) noted that one-dimensional model atmospheres will only work well if they have the same temporally- and spatially-averaged behaviour as the

species they are used to predict, which might not be the case for Li. Kurucz considered the idea that conventional abundance analysis is in error, and suggested that model atmospheres could underestimate the amount of ionized Li by an order of magnitude, which would lead to Li abundance measurements also being lower than the ‘true’ value by around 1 dex. Kurucz cautions us that “*since very few lines have atomic data known accurately enough to constrain the model, a match does not necessarily mean that the model is correct.*”

- Carlsson et al. (1994) studied the effect of non-local thermodynamic equilibrium (NLTE) on the formation of Li lines. They used a standard flux-constant plane-parallel atmosphere to model Li line formation, but included processes ignored by assumptions of local thermodynamic equilibrium (LTE). Inclusion of NLTE processes appears to have some effect on Li lines. NLTE corrections are largest for cool ($T_{\text{eff}} \sim 4500$ K), metal-poor ($[\text{Fe}/\text{H}] \sim -2$) objects, although the magnitude of the effect varies with both temperature and metallicity. Generally, the corrections have opposite signs for 6104 and 6708, increasing the abundance derived from the subordinate line by up to 0.06 dex (at $A(\text{Li}) = 2.2$) while decreasing it in the case of the resonance feature (by around 0.004 dex at $A(\text{Li}) = 2.2$ for an object with $T_{\text{eff}} = 6000$ K, $\log g = 4.0$, and $[\text{Fe}/\text{H}] = -2.0$).
- Stuik et al. (1997) continued the work of Carlsson et al., investigating the sensitivity of Li I and K I to activity in Pleiades stars. They stress that the variations in Li line strength in the Pleiades cannot be attributed to a spread in the stellar abundances until such time as the line-formation predictions and atmospheric models can be shown to be accurate. One test of this is the use of the potassium resonance line (which should not show any abundance spread as K is not expected to be depleted in these stars) as a proxy for Li. This line is formed in similar conditions and transitions to the Li resonance feature, and so should be affected similarly. Their results suggest that while Li and K are not sensitive to the direct effects of chromospheric activity, they can be strongly affected by temperature variations deeper in the stellar atmosphere, and by interactions between regions of different temperature stratification. Such effects are not included in the conventional one-dimensional models, and therefore might account for some of the effects seen. Pop. II stars should not be as active as young cluster objects, but there are likely to be similar (related or unrelated) omissions in our modelling of Pop. II stars. Kiselman (1997, 1998) used a 3-D solar-granulation snapshot to investigate the effects of departures from LTE in line formation on 6708. He reported marked line-strength variations over the granulation pattern for NLTE and LTE. He also produced syntheses of the line under these conditions

and compared them to solar observations, finding that calculations which included the detailed modelling of the line radiative transfer matched observations better than those which neglected it.

- Uitenbroek (1998) worked in a similar vein to Stuik et al. and Kiselman, considering the effect of convective surface inhomogeneities on the formation of the Li resonance line in the solar case. Uitenbroek uses 1.5- and two-dimensional NLTE calculations to investigate the effects of granulation on the lines. Again, granulation is unlikely to play a significant role in Pop. II-star Li modelling, but the fact that its omission in Pop. I models leads to a difference in abundance (although typically less than 0.1 dex) shows that our understanding of stellar atmospheres is not complete.
- BM98 detected 6104 in the Pop. II star HD 140283. This feature is important since it is formed deeper in the atmosphere than the resonance line, and can therefore be used to test our models, since both lines should present the same abundance. Bonifacio & Molaro’s analysis suggested that the same abundance could be used to adequately reproduce both lines using only 1-D, homogeneous models. They took this to imply that these ‘simple’ models were essentially correct.
- Asplund et al. (1999) have used 3-D, time-dependent surface-convection simulations of two Pop. II objects, HD 140283 and HD 84937 to investigate the effect of multi-dimensional modelling on Li abundance in metal-poor stars. They report that, as might be expected, three-dimensional model atmospheres have a different temperature structure to one-dimensional models. The effect of their 3-D, LTE models on the stellar Li is to decrease the abundance measured from the resonance line by 0.2-0.35 dex, relative to that obtained using 1-D models (for models with $T_{\text{eff}} = 5690$ K, $\log g = 3.67$, $[\text{Fe}/\text{H}] = -2.5$ and micro-turbulence (ξ) = 1 km s^{-1} in the case of HD 140283, and $T_{\text{eff}} = 6330$ K, $\log g = 4.04$, $[\text{Fe}/\text{H}] = -2.25$ and $\xi = 1 \text{ km s}^{-1}$ for HD 84937). Note that Asplund et al. 1999 quote $\log g$ for g in units of m s^{-1} ; for consistency with other works we use cm s^{-1} . However, 3-D NLTE corrections almost completely cancel the 3-D LTE effect, leading to < 0.1 dex change (in these two cases) to the 1-D LTE abundance (Asplund et al. 2000).

We seek here to extend the work of BM98. Firstly, their sample consists of only one star, which might or might not be typical of other Pop. II objects. Secondly, they do not fit 6104 independently of the resonance feature, but synthesize it at the abundance determined from the stronger feature. 6104 is difficult to measure due to its weakness and proximity to Fe and Ca lines. At the signal-to-noise ratio (S/N) of the BM98 spectrum it is likely that the 6104 Li abundance can only be determined to ± 0.2 dex (1σ). As this is comparable with the likely size of problems with the models and larger than the uncertainties claimed

by some authors in Li_p , a more sensitive comparison of 6708 and 6104 is desirable. Because of the weakness of the line, and difficulties achieving higher S/N , it is sensible to measure 6104 in a number of objects to reduce the statistical errors (see Sect. 4.1 and 4.2).

Following on from the work of BM98 we have obtained a larger sample of plateau stars (and three cooler objects) and analysed them with a variety of 1-D homogeneous models, fitting both lines independently of each other to determine if the abundances from the two lines do agree.

2. Observations and Reduction

Our sample consisted of 14 Pop. II stars taken from the larger sample of Bonifacio & Molaro (1997 – hereafter BM97) with $[\text{Fe}/\text{H}]$ from -1 to -2.8 , and temperatures in the range $5400\text{K} \leq T_{\text{eff}} \leq 6330\text{K}$ (as quoted by BM97). These are listed in Table 1.

Spectra were taken on the 4.2m William Herschel Telescope (WHT) on 1998 October 08 and 22, 1998 November 29, 1999 December 22-23, 2001 January 23-26 and 2001 April 26, on the 4m Anglo-Australian Telescope (AAT) on 1999 October 22, and 2001 April 26, and on the 8.2m Subaru Telescope on 2001 July 22. The Utrecht Échelle Spectrograph (on the WHT) and UCL Échelle Spectrograph (on the AAT) were used, both with E31 gratings, for their high resolving power ($R \sim 50000$). On the Subaru Telescope, the High Dispersion Spectrograph was used, configured for $R \sim 90000$. The usual calibration frames were taken in all cases, including tungsten flat fields, bias frames, and thorium-argon hollow-cathode-lamp spectra. The data were extracted and wavelength calibrated using the Starlink ECHOMOP (Mills et al. 1997) and FIGARO (Shortridge et al. 1999) packages for the WHT and AAT data, and IRAF for the Subaru data. Scattered-light subtraction was included in the data reduction. Several exposures of each target were taken and co-added to give a typical S/N of 250-350 per pixel, but very much higher quality data were obtained for HD 140283 (13 observations were taken, with a total exposure time of 4924 seconds), where we achieved $S/N = 1100$ per 0.018\AA pixel! The spectrum was heavily affected by fringing for wavelengths $> 7000\text{\AA}$, but this was not a problem in the region of the lithium lines.

These S/N values were determined from the RMS discrepancies arising from a polynomial fit to line-free spectral regions (as determined by a spectrum synthesis with appropriate T_{eff} and $[\text{Fe}/\text{H}]$ parameters). This estimate of S/N is likely to be representative, and up to $\sim 30\%$ smaller than S/N determined from the total number of counts for each object. Fig. 1 shows spectra in the region of 6708, while the 6104 spectra are presented in Fig. 2.

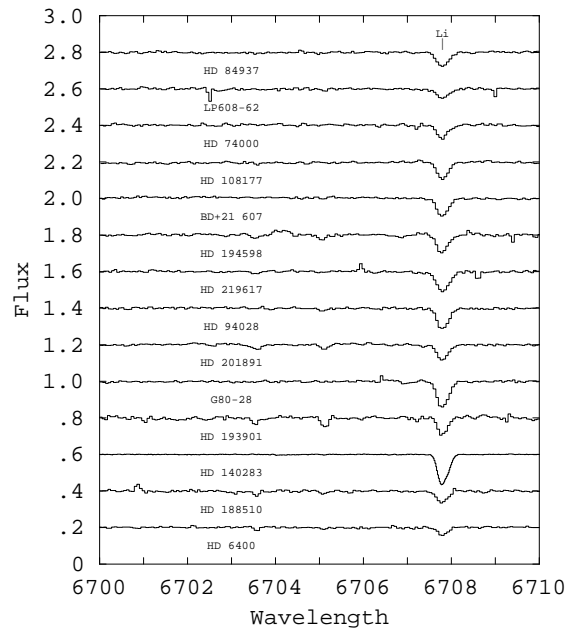


Fig. 1. Normalised spectra for our sample stars in the region of the 6708 line. The spectra have been vertically offset for clarity. Fe I lines at 6703\AA and 6705\AA can be seen in the more metal-rich objects.

3. Analysis

T_{eff} , $\log g$, and $[\text{Fe}/\text{H}]$ values were taken from BM97. These values are presented along with alternate identifiers in Table 1. A microturbulence of 1 km s^{-1} was used, as in BM97 and BM98. The analysis is virtually independent of the microturbulence value used; a change of $+0.5\text{ km s}^{-1}$ affects 6708 by less than 0.04 dex, and 6104 by less than 0.01 dex, for all objects in our sample. Initially a $v \sin i$ parameter of 5 km s^{-1} was used for all the objects, but this was varied until the best χ^2 value for the fit was obtained. We have used the $v \sin i$ parameter to model macroturbulent broadening of the lines, rather than as a physical rotational velocity. Instrumental broadening, determined by fitting Gaussians to arc lines, was also included in the syntheses. The values of both $v \sin i$ and instrumental broadening parameters used are included in Table 1. The models used were Kurucz 1-D, homogeneous, LTE, ATLAS9 model atmospheres with the mixing-length theory of convection (MLT – Castelli et al. 1997) with overshooting turned off.

Li abundances and EWs were determined by fitting a synthetic spectrum to the data using UCLSYN (Smith 1992, Smalley et al. 2001) and the line list in Table 3. The synthesis for 6708 included the weak Fe I line in the blue wing of the resonance feature. Given the low metallicities of these stars, the Fe line is unlikely to have a significant EW, but it was included for completeness. The abundances of Fe and Ca were determined from the lines near 6104 by fitting syntheses to them prior to fitting the Li line. The gf factors of these additional lines were fixed

Table 1. Identifiers, effective temperatures, surface gravities and metallicities for sample stars. Variations in S/N between the orders arise from different numbers of counts in each échelle spectral order and the presence of cosmic rays near the lines in some objects, resulting in fewer exposures being co-added for some objects. Note that the identifiers in bold are those used throughout this paper.

Star Identifier	Other	T_{eff}	$\log g$	[Fe/H]	S/N 6708	S/N 6104	$v \sin i^*$ (km s^{-1})	Run [†]	Notes		
HD 84937	G43-003	BD+14 2151	6330	3.90	-2.49	285	300	7	6	CS	
HD 83769C	G49-029	BD+01 2341	LP 608-62	6313	3.90	-2.81	240	220	5	6	Cs
HD 74000		BD-15 2546		6224	4.08	-2.00	230	249	7	5	
HD 108177	G13-035	BD+02 2538		6097	4.03	-1.98	250	250	5	6	s
HD 28428	G8-016	BD+21 607		6034	4.05	-1.61	220	430	6	6	s
HD 194598	G24-015	BD+09 4529		6017	4.15	-1.37	160	240	4.5	2	
HD 219617	G273-011	BD-14 6437		6012	4.30	-1.63	260	240	6.5	2,3,4	C
HD 94028	G55-025	BD+21 2247		6001	4.15	-1.50	270	270	4.5	3,5	S
HD 201891		BD+17 4519		5909	4.18	-1.22	285	250	4	2,3	S
HD 24289	G80-28	BD-04 680		5866	3.73	-2.07	250	330	5	6	
HD 193901		BD-21 5703		5750	4.40	-1.13	130	180	3.5	2,4	
HD 140283		BD-10 4149		5691	3.35	-2.37	1100	1100	4	7	
HD 188510	G142-017	BD-10 4091		5564	4.88	-1.80	250	255	2	2,3	CS
HD 64090	G90-025	BD+31 1684		5441	4.50	-1.82	300	370	1	3,5	

* $v \sin i$ has been used to model macroturbulence, and does not imply that the stars rotate at these speeds.

† The relevant Table 2 column numbers for each object.

Notes: C – classified as a binary or suspected binary by Carney (1983)

S – classified as a definite binary by Stryker et al. (1985)

s – classified as near significance criterion for binaries by Stryker et al. (1985).

Table 2. Observational information for data in this paper.

(1) Date	(2) 1998 Oct	(3) 1998 Nov	(4) 1999 Oct	(5) 1999 Dec	(6) 2000 Jan	(7) 2001 Jul
Telescope	WHT	WHT	AAT	WHT	WHT	Subaru
Detector	SITe1	SITe1	MITLL2	SITe1	SITe1	2×EEV
Pixel size (μm)	22.5	22.5	15	22.5	22.5	13.5
Dispersion ($\text{\AA}/\text{pixel}$)	0.05	0.05	0.05	0.06	0.05	0.02
Slit width	1.2"	1.3"	1.2"	1.4"	1.16"	0.4"
FWHM at 6104Å (Å)	0.12	0.12	0.12	0.16	0.13	0.07

by matching the lines in our observed and synthesized solar spectra. Best fits were determined by χ^2 minimization. The solar model used was: $T_{\text{eff}} = 5777\text{ K}$, $\log g = 4.44$, $\xi = 1.5\text{ km s}^{-1}$. The Li gf factors are those contained in the Vienna Atomic Line Database (VALD - Piskunov et al. 1995). The VALD data for 6104 is also identical to that presented by Lindgard & Nielsen (1977), which are accurate to within 10% for 6104, and within 3% for 6708. The Van der Waals broadening coefficients for the Fe I and Fe II, Ca I and Li I lines were those reported by Barklem et al. (2000 – hereafter ABO values).

6104 can be seen in the spectra of some of our sample (Fig. 2): HD 84937, BD+21 607, HD 194598, HD 219617, G80-28, HD 140283 and HD 188510 all show a feature at the appropriate wavelengths. For the other objects a 3σ upper limit was determined from the pixel size (p , in Å), S/N , and the physical width of the line (r , in Å) in other objects with similar atmospheric parameters such that:

Table 3. Lines used in spectral synthesis and analysis.

Element	Wavelength (Å)	Excitation Potential (eV)	$\log gf$
Fe I	6707.432	4.608	-2.357
Li I	6707.754	0.000	-0.431
Li I	6707.766	0.000	-0.209
Li I	6707.904	0.000	-0.773
Li I	6707.917	0.000	-0.510
Fe I	6102.159	4.608	-2.692
Fe I	6102.173	4.835	-0.454
Ca I	6102.723	1.879	-0.950
Fe I	6103.186	4.835	-0.721
Fe I	6103.294	4.733	-1.325
Fe II	6103.496	6.217	-2.224
Li I	6103.538	1.848	0.101
Li I	6103.649	1.848	0.361
Li I	6103.664	1.848	-0.599

$\sigma_{EW} = \frac{\sqrt{(rp)}}{S/N}$. The corresponding abundance limit was determined by performing a synthesis with $EW = 3\sigma_{EW}$.

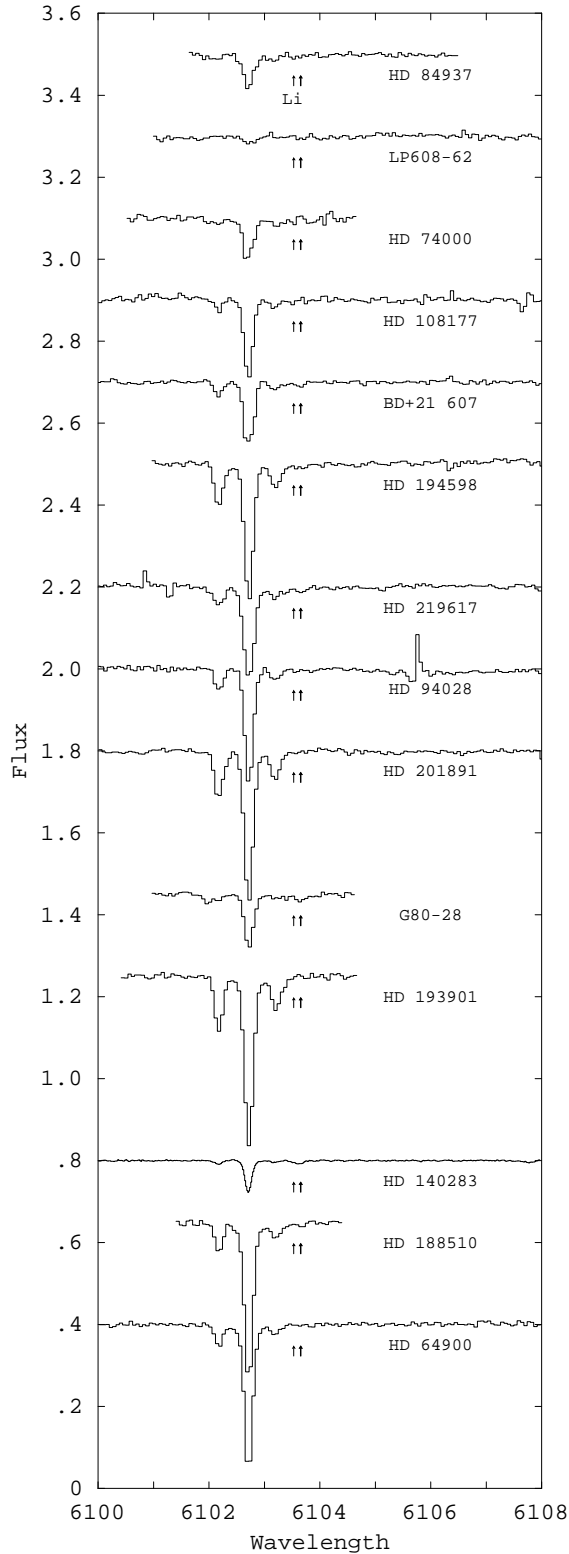


Fig. 2. Normalised spectra for our sample stars in the region of 6104. Arrows indicate the wavelengths of the 6104 triplet, which can be seen in **HD 84937**, BD+21 607, HD 194598, HD 219617, G80-28, HD 140283 and HD 188510. The spectra have been vertically offset for clarity.

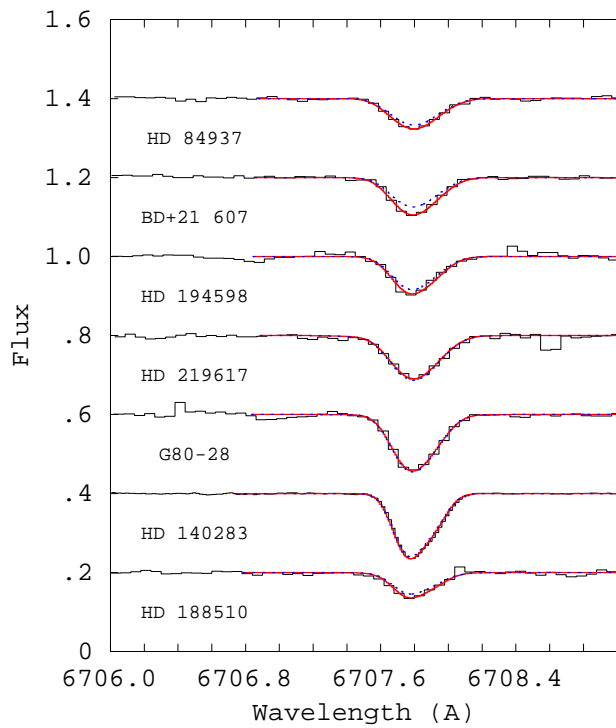


Fig. 3. Observed data (solid lines) and synthetic fits in the region of 6708, using our abundances (heavy lines) and the abundances reported in BM97 (dotted lines) for objects with 6104 detections. Spectra are vertically offset for clarity.

Figs. 3 and 4 show the detailed synthetic fits to the data in the 6708 and 6104 regions. Fig. 3 also shows the syntheses using our models and the abundances reported in BM97, which we discuss later in the paper.

4. Results

LTE Li abundance measurements or upper limits for all the objects in our sample are presented in Table 4, along with the synthetic EWs. We also corrected the LTE abundances for NLTE effects using the code of Carlsson et al. (1994), and these values are also presented in the table. At first glance the detections from 6104 appear higher than those from 6708, although there are upper limits where the abundances might agree. Before we can fully consider this as intrinsic to the stars, we need to consider possible sources of error which could account for the difference.

4.1. Atmospheric Uncertainties

Deblending is not likely to contribute significantly to the EW uncertainties, except perhaps in the most metal-rich objects in our sample. The main factor in determining the quoted errors is the S/N value adopted for each obser-

Table 4. Li EWs and abundances for sample objects derived from 6708 and 6104.

Object	EW ₆₇₀₈ $\pm \sigma$ (mÅ)	A(Li) ₆₇₀₈ $\pm \sigma$ LTE	A(Li) ₆₇₀₈ NLTE	EW ₆₁₀₄ $\pm \sigma$ (mÅ)	A(Li) ₆₁₀₄ $\pm \sigma$ LTE	A(Li) ₆₁₀₄ NLTE
HD 84937	26.67 \pm 0.78	2.36 \pm 0.01	2.30	2.24 \pm 0.77	2.46 $^{+0.13}_{-0.18}$	2.50
LP 608-62	16.71 \pm 1.01	2.09 \pm 0.03	2.07	\leq 1.98	\leq 2.41	\leq 2.46
HD 74000	22.22 \pm 0.90	2.18 \pm 0.02	2.18	\leq 1.93	\leq 2.37	\leq 2.42
HD 108177	29.81 \pm 0.98	2.23 \pm 0.02	2.22	\leq 1.80	\leq 2.28	\leq 2.32
BD+21 607	31.55 \pm 0.83	2.23 \pm 0.02	2.23	2.62 \pm 0.68	2.44 $^{+0.10}_{-0.13}$	2.50
HD 194598	30.28 \pm 0.81	2.21 \pm 0.02	2.21	2.55 \pm 0.94	2.43 $^{+0.14}_{-0.20}$	2.49
HD 219617	38.28 \pm 0.60	2.31 \pm 0.02	2.30	3.36 \pm 0.67	2.54 $^{+0.08}_{-0.10}$	2.60
HD 94028	36.51 \pm 0.88	2.29 \pm 0.02	2.29	\leq 1.61	\leq 2.21	\leq 2.27
HD 201891	26.31 \pm 0.83	2.07 \pm 0.02	2.08	\leq 1.74	\leq 2.21	\leq 2.28
G80-28	46.21 \pm 0.52	2.28 \pm 0.01	2.29	4.41 \pm 0.60	2.57 $^{+0.06}_{-0.06}$	2.65
HD 193901	26.48 \pm 1.75	1.96 \pm 0.03	1.99	\leq 3.45	\leq 2.47	\leq 2.53
HD 140283	48.10 \pm 0.11	2.157 \pm 0.002	2.19	1.81 \pm 0.15	2.09 $^{+0.04}_{-0.04}$	2.19
HD 188510	20.41 \pm 0.56	1.69 \pm 0.02	\star 1.74	2.08 \pm 0.63	2.17 $^{+0.12}_{-0.16}$	\star 2.23
HD 64090	12.05 \pm 0.92	1.32 \pm 0.03	1.38	\leq 1.68	\leq 1.96	\leq 2.06

* The log g values for HD 188510 are out of range for the NLTE-correction script, so a log g of 4.5 was used. This is likely to make a difference of \leq 0.01 dex in abundance from either line.

vation, in that those objects with low S/N have larger errors or EW upper-limit predictions. There appears to be a small spread in abundances from both lines (covering a range of 0.4 dex for 6708 and \geq 0.4 dex for 6104, neglecting stars cooler than 5800 K). We caution the reader that the uncertainties reported and plotted are purely those intrinsic to the S/N and the modelling/synthesis processes, determined by requiring the reduced- χ^2 value to increase by 1, or the values from $\frac{\sqrt{(rp)}}{S/N}$ if greater (only the latter estimate is used where there is no detection of the line). They do not include contributions for uncertainties in photometry, T_{eff} , log g , [Fe/H], or other parameters. Of these only the temperature error is likely to be significant, with a 100 K increase in temperature raising the abundance by 0.07 dex for 6708, or 0.04 dex for 6104 (for a 6000 K star with log g = 4.0, [Fe/H] = -2.0 and A(Li) = 2.17). This would introduce an additional uncertainty of \pm 0.03 dex into the relative abundance from the two lines at 6000 K, growing to 0.05 dex at 5000 K. A 0.5 dex change in log g will raise the abundance by $<$ 0.01 dex for both lines; increasing [Fe/H] by 0.5 dex will only increase the abundance by \sim 0.02 dex. Neither of these can induce a large systematic discrepancy in the abundances measured from the two lines. BM97 report that a 0.5 km s $^{-1}$ change in microturbulence will alter the abundance by only 0.005 dex. Since the main aims of this work are to compare the abundances from the two lines, and to compare our results to those of BM97 and BM98 using *their* model parameters, the errors we have obtained should be sufficient. If our data are to be compared to those of other authors, the additional uncertainties should be taken into account.

4.2. Atomic Parameter Uncertainties

There will also be uncertainties due to the atomic parameters used, e.g. oscillator strengths. The errors in the gf values we have used propagate to abundance differences of \sim 0.01 dex for 6708 and \sim 0.04 dex for 6104, leading to a differential uncertainty of \sim 0.04 dex. For the purpose of comparing our data with that of BM97, these are unlikely to be important since we have used essentially the same line lists. Broadening parameters (e.g. Stark and collisional broadening factors) will probably vary between this analysis and others since we have used the ABO collisional broadening factors (Barklem et al. 2000) for the Fe, Ca and Li lines. The Stark factors are less important for lines which form in the outer layers of the atmosphere, as the Li lines do. The effect of using the ABO values rather than others is of order -0.01 dex for objects with $T_{\text{eff}} = 5000$ -6000 K and [Fe/H] = -2.0. We are content that for the purposes of comparing our data with that of Bonifacio & Molaro, and indeed other authors, our atomic data are satisfactory.

4.3. Comparison with data presented by Bonifacio & Molaro (BM97)

Table 5 contains 6708 results from both this paper and BM97.

There is no systematic trend between either our EWs or abundances and those determined by BM97. All our results agree within 3σ , and most within 2σ . This is not surprising; the main difference between the two analyses, besides the different spectra, is BM97's use of α -enhanced opacities (with the α -process elements – O, Ne, Mg, Si, S, Ar, Ca and Ti – enhanced by 0.4 dex) which they suggest are more realistic for Pop. II stars; we used solar-scaled (non-enhanced) opacities as these were more readily avail-

Table 5. Synthetic EWs and LTE-derived abundances for 6708 from this paper and BM97.

Object	This paper		BM97	
	EW	A(Li)	EW	A(Li)
HD 84937	26.67±0.78	2.36±0.01	24.0±1.2	2.26±0.03
LP 608-62	16.71±1.01	2.09±0.03	22.0±2.3	2.20±0.05
HD 74000	22.22±0.90	2.18±0.02	25.0±3.4	2.22±0.02
HD 108177	29.81±0.98	2.23±0.02	32.0±1.3	2.26±0.02
BD+21 607	31.55±0.83	2.23±0.02	25.0±2.2	2.11±0.05
HD 194598	30.28±0.81	2.21±0.02	28.0±0.9	2.15±0.02
HD 219617	38.28±0.60	2.31±0.02	40.0±1.3	2.33±0.02
HD 94028	36.51±0.88	2.29±0.02	35.0±1.3	2.25±0.02
HD 201891	26.31±0.83	2.07±0.02	24.0±0.8	2.00±0.02
G80-28	46.21±0.52	2.28±0.01	47.0±2.1	2.29±0.03
HD 193901	26.48±1.75	1.96±0.03	30.0±3.4	1.98±0.06
HD 140283	48.10±0.11	2.16±0.01	47.5±0.6	2.14±0.05
HD 188510	20.41±0.56	1.69±0.02	18.0±3.4	1.60±0.10
HD 64090	12.05±0.92	1.32±0.03	12.0±1.0	1.30±0.04

able. We have determined that the difference in opacities affects the abundances of both lines by less than 0.03 dex at 5000 K (for a model with $\log g = 4.0$, $[\text{Fe}/\text{H}] = -1$, $\xi = 2 \text{ km s}^{-1}$, and $\text{EW}_{6104} = 5 \text{ m}\text{\AA}$ or $\text{EW}_{6708} = 132 \text{ m}\text{\AA}$), or less than 0.01 dex at 6000 K (models as previous), with the α -enhanced opacities reducing the derived abundances relative to the non-enhanced models. This is comparable to the differences between some of our values and those of BM97, although for other objects our abundances are smaller. We note that BM97 have taken the EWs published in several other surveys, averaged them where appropriate, and re-determined the Li abundances. They do not list which objects have been taken from which source, or how many observations have been averaged to produce each EW, so it is impossible to tell if any of the surveys used has provided systematically larger EWs than any other. They also report that EW measurements might be affected by non-Gaussian noise, such as scattered light, but do not mention what steps have been taken (if any) to minimise the impact of these effects, bearing in mind that they will also vary from sample to sample. Neglect of scattered-light correction would result in the lines being partially ‘filled in’, reducing the observed EW and thus the derived abundances. RNB99 also commented on the non-uniformity of the sample, noting that the inhomogeneity of the sample would have contributed to the spread observed in their results. We are confident that our homogeneous and consistent data reduction and analysis provide satisfactory results from 6708.

5. Discussion

5.1. 6104 versus 6708

Using consistent reduction and analysis techniques, we have measured 6104 in seven of our fourteen Pop. II stars and obtained upper limits in the others. We have measured 6708 in all the objects.

There is evidence of a discrepancy in Li abundance between the two lines for some of our sample objects. In Fig. 5 which plots our 6104 abundances *versus* those from 6708, it appears that the 6104 abundances of some objects (e.g. HD 219617 and G80-28) are higher than those from 6708. Figure 5 might also give the impression that we have uncovered a systematic discrepancy between the 6104 and 6708 abundances. However, part of this is due to the large number of upper limits, which make it impossible to draw such a conclusion. Indeed, as we describe below, there are some objects for which a large discrepancy can be ruled out. The discrepancy between 6104 and 6708 abundances is most apparent, reaching ~ 0.5 dex, at low values of A(Li) where, admittedly, there is more potential for overestimation of the 6104 equivalent width. At higher abundances the points lie closer to the one-to-one relation, but several are still $\sim 2\sigma$ above it.

A measurement of the 6104 line is more likely to be made not only in objects where the line *is* stronger, but also when noise acts to make it *appear* stronger. Because of this latter bias, it is not surprising that *some* of the 6104 abundances exceed those of 6708. Nevertheless, it is disquieting that in three of the fourteen cases, the abundance obtained from the 6104 line exceeds that from 6708 by more than twice the formal error, *i.e.* $> 2\sigma$. This can be seen in Fig. 4: the 6708 abundance clearly *does not* fit the observations in some cases, most notably for HD 219617 and G 80-28. If the error distribution was Gaussian, and our error estimates were reliable, there would be only 2% probability of a 6104 abundance exceeding that from 6707 by 2σ . This would give rise to fewer than one discrepant case in fourteen. However, there are also cases where such discrepancies cannot exist: HD 140283 (discussed below), HD 108177 and HD 94028 all have 6104 abundances which are consistent with the 6708 abundances. Overall, this leads to a very mixed picture where the abundances from the two lines agree for some objects, some objects

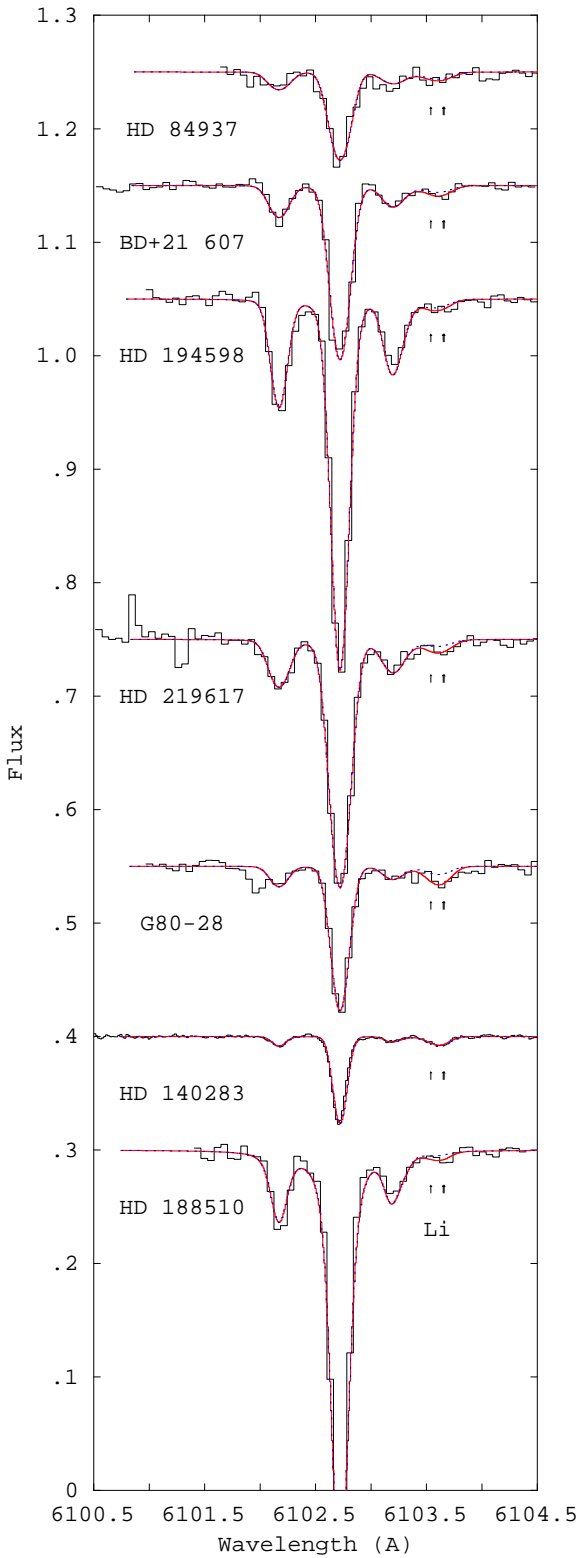


Fig. 4. Observed data (histogram) and synthetic fits in the region of 6104, using our abundances (heavy lines) for objects with 6104 detections. Syntheses using the 6708 abundance are also shown (dashed lines). Spectra are vertically offset for clarity, and arrows indicate the position of the Li-triplet components (the arrows for 6103.65 and 6103.66 are superimposed).

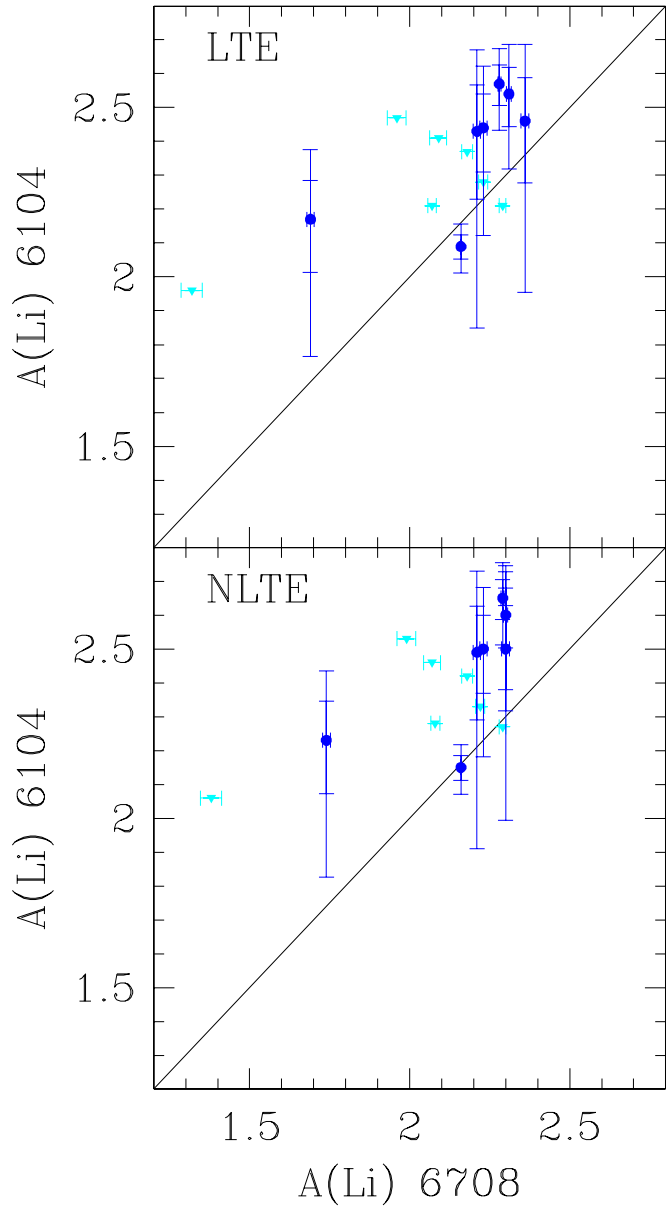


Fig. 5. $A(\text{Li})_{6104}$ versus $A(\text{Li})_{6708}$ for sample stars. The solid line is the 1-to-1 relation. Since error bars which are linear in EW become non-linear in $A(\text{Li})$, especially for a line as weak as 6104, we show both 1σ and 2σ error bars for the abscissa. Upper limits are shown as inverted triangles. *Upper panel:* LTE abundances. *Lower panel:* NLTE abundances.

have $A(\text{Li})_{6104} > A(\text{Li})_{6708}$, and some objects might have $A(\text{Li})_{6708} > A(\text{Li})_{6104}$ (although the latter possibility is defined by only one object in our sample; the other upper limits neither contradict nor constrain this possibility). The lack of a clear picture of what is going on adds a further complication into any interpretation of the data,

in that whatever causes the elevated 6104 abundances in some stars is not present in other objects.

We have plotted the abundances for the two lines against T_{eff} and [Fe/H] in Fig. 6. In the case of the A(Li)-versus- T_{eff} plot, the plateau can be seen for both lines, with similar abundances for objects with $T_{\text{eff}} \geq 5800$ K. The 6104 abundances appear to show a separate plateau $\lesssim 0.5$ dex above the 6708 plateau. As with Fig. 5, this impression is accentuated by the high number of upper limits, especially at low temperature, but concentrating only on the firm detections shows that the discrepancy is not an obvious function of effective temperature or metallicity. The Li abundances in the plateau objects all appear approximately constant with metallicity, although slopes in either direction could potentially be present. The behaviour of objects at the cool edge of the plateau is much as expected, with Li abundances from both lines decreasing with decreasing temperature, consistent with HD 188510 and HD 64090 being cool enough that some Li depletion is likely to have occurred during their lifetimes.

In order to investigate the abundance disparity further, more firm detections would be needed, although obtaining them is complicated by the increased difficulty in measuring such weak 6104 lines. Achieving higher S/N exceeding a few hundred not only requires longer and longer exposures, but also requires highly repeatable flat-fields that correct for fringing and other defects to better than 0.1%.

5.2. HD 140283

The data for HD 140283 do not show a discrepancy between the 6104 and 6708 abundances. We also used our models to obtain abundances for HD 140283 using the EWs and model parameters quoted in BM97 and BM98. In contrast to the general behaviour noted in Sect. 5.1, we find $A(\text{Li})_{6708} = 2.16 \pm 0.01$ (from $\text{EW}_{6708} = 47.5 \pm 0.6 \text{ m}\text{\AA}$), slightly higher than $A(\text{Li})_{6104} = 2.10^{+0.07}_{-0.08}$ (from $\text{EW}_{6104} = 1.8 \pm 0.3 \text{ m}\text{\AA}$) but in any case in agreement within the errors. The abundance reported by BM98 for both lines in HD 140283 is $A(\text{Li}) = 2.14 \pm 0.13$, which is also in agreement with our calculated abundances.

Our observation HD 140283 allows us to compare our results for this object directly with that obtained by BM98. The main differences between our analysis and theirs are: the significantly-higher S/N of our spectrum (~ 1100 per 0.018\AA pixel, compared to BM98's 360 per 0.04\AA pixel); the gf values used in the syntheses (see Table 3 for our values, and Sect. 2 of BM98); their use of α -enhanced opacities versus our use of standard opacities (Sect. 4.3); our use of ABO broadening parameters. We have also included an Fe II line in our synthesis of the 6104 region, although at the metallicity of the object this should make no difference. The analyses shared identical T_{eff} , $\log g$, [Fe/H], ξ and $v \sin i$ values. Despite the differences between the analyses, we have obtained abundances which are completely consistent with those reported by

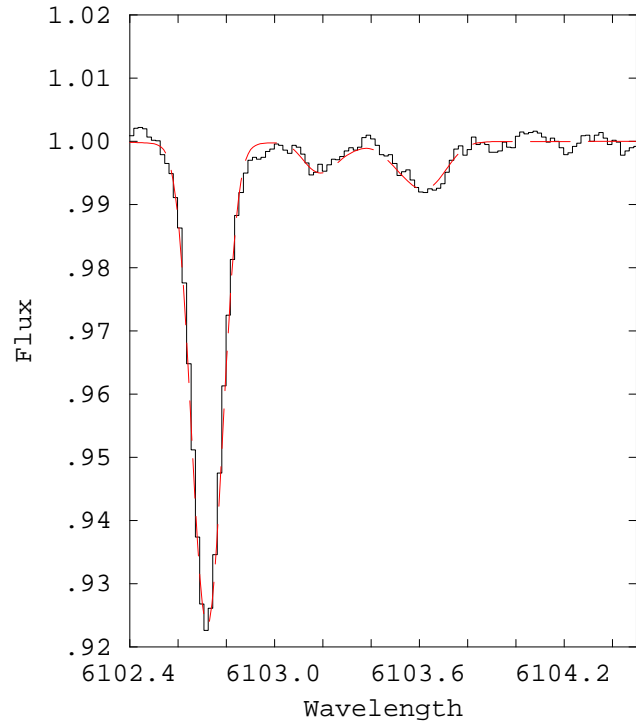


Fig. 7. Observed (solid) spectrum and synthetic fit (dashed) to 6104 in HD 140283.

BM98, which is not too surprising since the differences are all in parameters which have only a small effect on abundance. Even so, it shows that there is a good degree of consistency between the two studies. Our fits to both 6708 and 6104 are remarkably close to the observations (Figs. 3 and 7), suggesting that our line profiles are reliable.

In concluding this subsection, we reemphasize that the 6104 lines are all very weak, and it is possible that we have underestimated the errors, but we discuss below the implications of a genuine discrepancy.

5.3. Model atmospheres

If the possible discrepancy between the 6104 and 6708 lines in some of the objects is real, what could explain it? Errors in T_{eff} of ± 100 K lead to abundance *differences* between 6708 and 6104 of ± 0.03 dex at 6000 K, and ± 0.05 dex at 5000 K, with 6708 abundances changing more than 6104 abundances. This has already been shown to be too small; a 1000 K temperature increase would be required to bring the most discrepant lines into agreement (see Sect. 4.1), and the inclusion of other model uncertainties contributes less than 0.03 dex.

An alternative explanation for our result is that the model atmospheres do not adequately represent the stars we are studying, and a change in temperature gradient

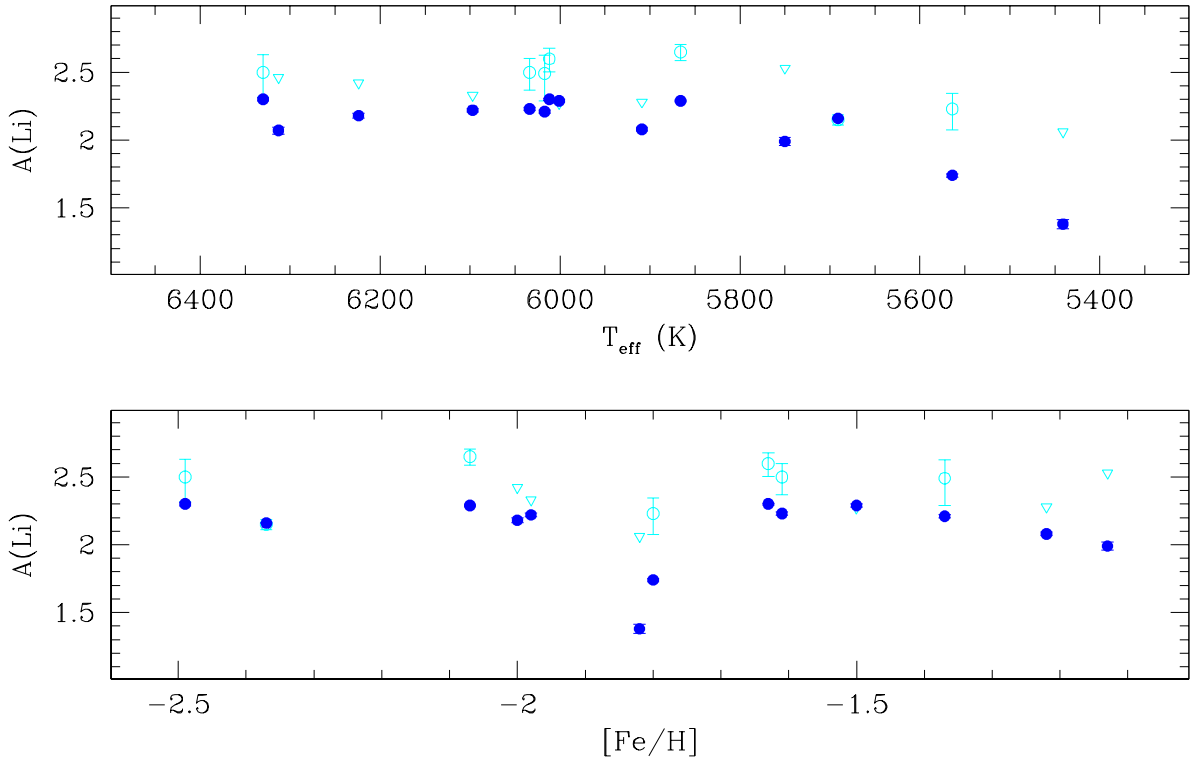


Fig. 6. NLTE-corrected $A(\text{Li})$ versus T_{eff} (upper panel) and $[\text{Fe}/\text{H}]$ (lower panel) for sample stars. Filled symbols represent 6708 abundances and open symbols show 6104 values. Inverted triangles indicate 6104 upper limits.

within the stellar atmospheres might explain our observations. Asplund et al. (1999) applied 3-D model atmospheres to two Pop. II stars, HD 140283 and HD 84937, noting the predicted effect on the Li abundances relative to those from 1-D models. 3-D models alter the temperature stratification in a stellar atmosphere, with the greatest variations between 1-D and 3-D models occurring at the inner and outer boundaries (see lower panel of Fig. 8). The upper panel of Fig. 8 shows the flux contribution functions $d(F_{\nu})/d\log_{10}(\tau_{5000})$ computed for four wavelengths in the spectrum of HD 140283, using our model atmosphere. These show the range of depths over which the spectrum forms at a given wavelength (e.g. Gray 1992, Chapter 13). The greater equivalent width of 6708 and its lower excitation potential both lead to it forming on average further out than 6104.

The temperature differences between the 1-D and 3-D models of Asplund et al. are fairly small at optical depths between $\frac{1}{30} < \tau_{5000} < \frac{2}{3}$. However, the lower temperatures of the 3-D models beyond this range, where part of the flux at 6708 emerges, result in a stronger line forming in the 3-D models. (Switching to a 3-D model would also modify the contribution function from that shown). Asplund et al. found that, for a given EW, the 6708-derived abundance in HD 140283 would be 0.34 dex lower if derived using 3-D LTE models rather than 1-D LTE atmospheres.

Although 6104 could also be affected by the differences between 1-D and 3-D models, 6104 is so weak ($\text{EW} = 1.8 \text{ m}\text{\AA}$) that it is barely distinguishable from the neighbouring continuum, and the magnitude of the effect is probably less for this line. Asplund (priv. comm.) confirms this expectation. In this case, use of 3-D LTE models would decrease the 6708 abundance more than the 6104 abundance, *increasing* the abundance discrepancy identified in Sect. 5.1 (if it is real) between the two lines.

1-D NLTE effects, which have been corrected for in our results, have been discussed in three other studies of low-metallicity stars, namely Kurucz (1995), BM98, and Molaro et al. (1995). As can be seen from our Fig. 5 the NLTE corrections are relatively small, affect both lines differently, and vary depending on temperature, metallicity and Li abundance. In all cases, however, application of the NLTE correction acts to *increase* the 6708 and 6104 abundance difference, rather than reducing it.

Asplund et al's (1999) suspicion that overionisation of Li in 3-D models might reverse the 0.3 dex difference initially found for the 6708 line between the 1-D LTE and 3-D LTE models proved to be correct (Asplund 2000). However, corrections for overionisation may be expected to affect both the 6104 and 6708 lines, though not necessarily equally (due to the different depths of formation). It is clear that detailed calculations using 3-D NLTE atmo-

spheres will be required for each programme star to fully evaluate the competing effects and their different action on the two lines.

To produce the discrepancy via temperature gradients alone, what would be required is a process which changes the temperature gradient in opposite ways for the two lines, such that it increases the temperature in the outer region where 6708 is formed, thus weakening that line and leading to an underestimate of its abundance, and decreasing the temperature in the deeper region where 6104 forms. As noted above, this is opposite to the behaviour seen in the 3-D atmospheres of Asplund et al. (1999).

5.4. Binarity

There are no clear systematic effects of binarity on Li abundances derived from either line. Of our seven detections, three are in objects classified as binaries by Carney (1983): HD 84937, HD 219617 and HD 188510; both HD 84937 and HD 188510 have also been classified as definite binaries by Stryker et al. (1985). One object in our sample, BD+21 607, is near the significance criterion for binarity (Stryker et al. 1985), and the remaining three have not been classified as binaries by either study. The upper limits do nothing to clarify the picture with respect to binarity either: LP 608-62, HD 94028, HD 108177 and HD 210891 have all been classified as either definite or probable binaries by Carney or Stryker et al., while the remainder are probably not binaries. Clearly some other solution is required to explain the abundance discrepancy between the two lines.

5.5. Contrast with Pop. I stars

In a related paper (Ford et al. 2002) we found evidence that 6104 gave higher Li abundances than 6708 for some young Pleiades G/K dwarfs, whilst for others there seems to be reasonable agreement. This is very similar to the situation we find here for Pop. II stars.

For the Pleiades stars we were able to bring the abundances estimated from the two lines into agreement by introducing cool starspots into the atmospheric models. We did this in a simple way, by modelling the atmosphere as two one-dimensional components with differing temperatures and surface areas. In young Pop. I stars there is plenty of evidence (from Doppler imaging and light-curve modulation) that such spots exist, and so it is sensible to incorporate them in the models. Our conclusion was that plausible spot coverages and temperatures could explain the abundance discrepancies we saw in one-component models, although we had insufficient data to determine whether the stars actually did possess spots with the right properties.

We do not expect to find large, magnetically-generated spot regions associated with Pop. II stars. They are old, have spun down and their convection zones are much thin-

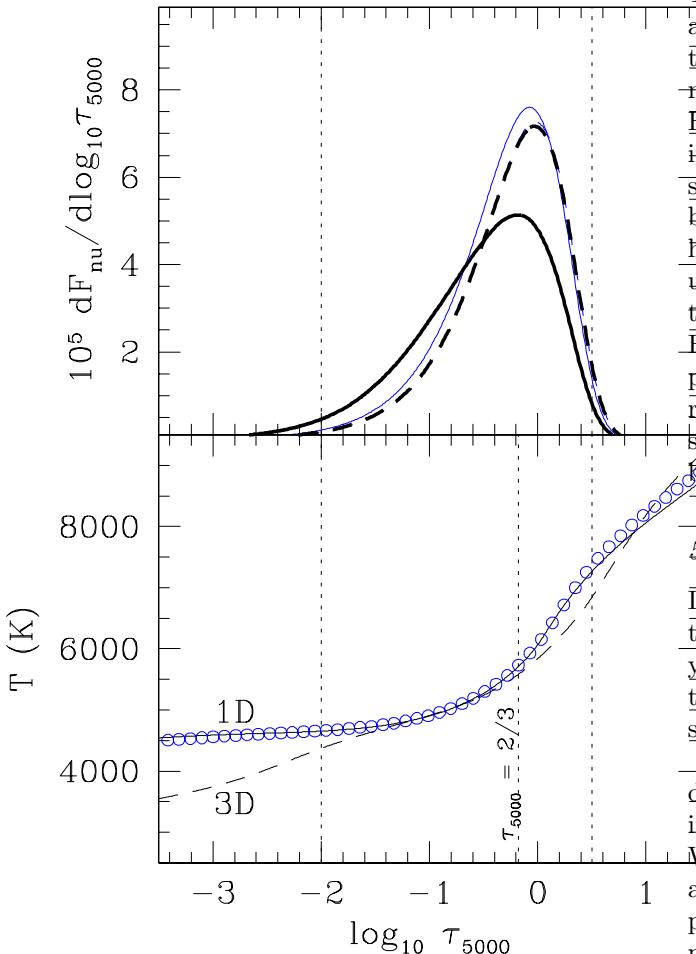


Fig. 8. *Upper panel:* Flux contribution functions for our 1-D model of HD 140283, which shows the range of depths over which the spectrum forms. Shown are contributions functions for the continuum near 6708 Å (thin solid curve), the Li 6708 line (heavy solid curve), the continuum near 6104 Å (thin dashed curve), the Li 6104 line (heavy dashed curve). (The contribution function plotted for each spectral line is a weighted average of the contribution functions at several wavelengths within the line profile.) *Lower panel:* Temperature profiles for our 1-D model (open circles) and 3-D model (solid line) for HD 140283. The slope $2/3$ is indicated.

ner than the Pop. I objects we considered in the Pleiades. For these reasons we do not think it appropriate to consider cool starspots as an explanation for the abundance discrepancies we see in Pop. II stars. That we still see a discrepancy (in some but not all stars) in Pop. II objects is likely to be an indication that something else is still wrong with our atmospheric models. It may also be the case that these additional problems are also present in Pop. I stars, and that the starspot interpretation is only part of the story. Indeed, even after the introduction of starspots on to the Pop. I stars we were unable to reduce the large dispersion that is seen in their Li abundances.

5.6. Effects on cosmological parameters: η and Ω_B

If we consider that the 6104-derived abundances are less likely to be affected by multi-dimensional model-atmosphere variations than those from 6708, then the plateau abundance inferred from our 6104 *detections* would be $A(\text{Li}) \sim 2.5$. (We do not include possible depletion factors in the values quoted below, although our 6104 abundance is the same as that derived by Salaris & Weiss (2001) from their diffusion models, constrained by observations of 6708). This would lead to two possible values for the baryon-to-photon ratio (η : values given here are $\eta_{10} = 10^{10}\eta$) of either ~ 1.0 or ~ 7.0 , leading to values of $3.7 \times 10^{-3}h_o^{-2}$ or $25.5 \times 10^{-3}h_o^{-2}$ for Ω_B , the Universal baryon density (where $h_o = \frac{H_o}{100} \text{ km s}^{-1} \text{ Mpc}^{-1}$ and the microwave background temperature is 2.73 K). Values for $A(\text{Li})_{\text{plateau}} = 2.09$ (Ryan et al. 2000) would be: $\eta_{10} \sim 1.2$ or 6.0 ; $\Omega_B \sim 4.4 \times 10^{-3}h_o$ or $21.9 \times 10^{-3}h_o^{-2}$, with the ~ 0.4 dex change in $A(\text{Li})$ affecting Ω_B by $\sim 16\%$. In either case, this assumes that the plateau abundance is indicative of the primordial Li abundance. However, this assumption may be unsound. The work of RNB99 found that the plateau slopes with metallicity, suggesting that the material from which the stars formed was gradually being metal enhanced over the time when Pop. II objects were being created. Despite the difficulties in measurement of weak lines, abundances from low-metallicity stars, which we assume to have formed earliest, still provide the best starting point for determinations of Li_p and related cosmological parameters.

6. Summary

We have obtained data for a sample of 14 Pop. II stars with high signal-to-noise ratios, which were all consistently reduced and analysed.

- We measured the 6708Å Li I resonance line in all our sample objects. We compared our EWs and abundances with those of Bonifacio & Molaro (BM97), finding good agreement between the values at a 99% confidence level.

- We also measured the 6104Å Li I subordinate line in seven of the stars, obtaining upper limits for the rest of the sample;
- Abundances from the 6104Å line hinted at a systematically higher Li abundance than those from the 6708Å line, with some stars discrepant by up to ~ 0.5 dex, while in others the discrepancy is no larger than ~ 0.1 dex. This trend was very weak, and a large preponderance of upper limits prevent any firm conclusions from being drawn;
- This difference cannot be explained by including NLTE-corrections, which actually make the discrepancy larger. Binarity does not appear likely to affect the abundance difference;
- The 3-D model results of Asplund et al. (1999) for Pop. II stars HD 84937 and HD 140283 suggest that the use of multi-dimensional atmosphere models would most likely increase any abundance discrepancy between the lines relative to that inferred from one-dimensional models. Our results can be used to place strong constraints on the 3-D modelling of these stars, perhaps indicating areas where further improvements could be made (e.g. improved NLTE-modelling, inclusion of magnetic fields). As they stand, however, we do not believe that 3-D models can explain our results.

Acknowledgements. The William Herschel and Isaac Newton Telescopes are operated on the island of La Palma by the Isaac Newton Group in the Spanish Observatorio del Roque de los Muchachos of the Instituto de Astrofísica de Canarias. The AAO operates the Anglo-Australian and UK Schmidt telescopes on behalf of the astronomical communities of Australia and the UK. To this end the Observatory is funded equally by the Australian and British Governments. Subaru is an 8.2 meter optical-infrared telescope at the summit of Mauna Kea, Hawaii, operated by the National Astronomical Observatory of Japan (NAOJ) with the support of the Ministry of Education, Culture, Sports, Science, and Technology. We extend our gratitude to Martin Asplund for his helpful advice and comments, and for kindly providing data for Fig. 8. SGR was supported by grant PPA/0/S/1998/00658 from the UK Particle Physics and Astronomy Research Council (PPARC). DJJ thanks the PPARC for a post-doctoral research fellowship, and the Royal Society for a European research grant. DJJ would like to acknowledge the continued positive influences of Mrs J. Pryer. The authors acknowledge the travel and subsistence support of PPARC. AF and JRB were funded by PPARC postgraduate studentships. Computational work was performed on the Keele, Open University and St Andrews nodes of the PPARC-funded Starlink network. This research has made extensive use of NASA's Astrophysics Data System Abstract Service.

References

Asplund, M., Nordlund, Å., Trampedach, R. & Stein, R.F. 1999, A&A, 346, L17
 Asplund, M. 2000, The Light Elements and Their Evolution, IAU Symp. 198, L. da Silva, M. Spite, & J.R. Medeiros (eds.), San Francisco ASP, 448

Barklem, P., Piskunov, N. & O'Mara, B. 2000, A&AS, 142, 467

Bonifacio, P. & Molero, P. 1997, MNRAS, 285, 847,

Bonifacio, P. & Molero, P. 1998, ApJ, 500, L175

Carlsson, M., Rutten, R.J., Bruls, J.H.M.J. & Shchukina, N.G. 1994, A&A, 288, 860,

Canuto, V.M. & Mazzitelli, I. 1991, ApJ, 270, 295

Canuto, V.M. & Mazzitelli, I. 1992, ApJ, 389, 724

Carney, B.W. 1983, AJ, 88, 623

Castelli F., Gratton, R.G. & Kurucz, R.L. 1997, A&A, 318, 841

Ford, A., Jeffries, R. & Smalley, B. 2002, in press.

Gray, D. F. 1992, The Observation and Analysis of Stellar Photospheres, 2nd edn (Cambridge: CUP)

Lindgard, A. & Nielsen, S. 1977, Atomic Data and Nuclear Data Tables, 19, 533

Kiselman, D. 1997, ApJ, 489, L107

Kiselman, D. 1998, A&A, 333, 732

Kurucz, R. 1995, ApJ, 452, 102,

Mills, D., Webb, J., Clayton & M. 1997, Starlink User Note 152.4

Molero, P., Primas, F. & Bonifacio, P. 1995, A&A, 295, L47

Pinsonneault, M.H. 1997, ARA&A, 35, 557

Pinsonneault, M.H., Walker, T.P., Steigman, G. & Narayanan, V.K. 1999, ApJ, 527, 180

Piskunov, N. E., Kupka, F., Ryabchikova, T. A., Weiss, W. W. & Jeffery, C. S. 1995, A&AS, 112, 525

Russell, S. 1996, ApJ, 463, 593

Ryan, S.G., Beers, T.C., Deliyannis, C.P. & Thorburn, J.A. 1996, ApJ, 458, 543

Ryan S.G., Norris, J.E. & Beers, T.C. 1999, ApJ, 523, 654

Ryan, S.G., Beers, T.C., Olive, K.A., Fields, B.D. & Norris, J.E. 2000, ApJ, 530, L57

Salaris, M. & Weiss, A. 2001, A&A, 376, 955

Shortridge, K., Meyerdieriks, H. & Currie, M. et al. 1999, Starlink User Note 86.17

Soderblom, D.R., Jones, B.F., Balachandran, S. et al. 1993a, AJ, 106, 1059

Smalley, B., Smith, K. & Dworetsky, M. 2001, UCLSYN User Guide, incorporating BINSYN and TELSYN, 3.1 edition

Smith, K. 1992, PhD thesis, University of London

Spite, F. & Spite, M. 1982, A&A, 115, 357,

Stryker, L.L., Hesser, J.E., Hill, G., Garlick, G.S. & O'Keefe, L.M. 1985, PASP, 97, 247

Stuik, R., Bruls, J.H.M.J. & Rutten, R.J. 1997, A&A, 322, 911,

Théado, S. & Vauclair, S. 2001, A&A, 375, 70

Uitenbroek, H. 1998, ApJ, 498, 427